Properties of $N = 90$ isotones within the mean field perspective

E. Ganioğlu,[1,*] R. Wyss,[2] and P. Magierski[3]
[1]*Science Faculty, Physics Department, Istanbul University, TR-34459, Istanbul, Turkey*
[2]*Department of Physics, KTH (Royal Institute of Technology), SE-10691 Stockholm, Sweden*
[3]*Faculty of Physics, Warsaw University of Technology, ulica Koszykowa 75, 00-662 Warsaw, Poland*
(Received 9 August 2013; published 14 January 2014)

In recent years, the $N = 90$ isotones have been investigated to a large extent in relation to studies of quantum phase transitions. In this paper, we use the mean field approach with pairing-deformation self-consistent total Routhian surface (TRS) calculations to study the $N = 90$ isotones and neighboring nuclei. The important probes, such as moments of inertia, quadrupole moments, the energy ratio of $E(4_1^+)/E(2_1^+)$, and octupole and hexadecapole degrees of freedom are considered and the calculated results are compared with the available experimental data. From a microscopic point of view, the $N = 90$ isotones characterize the onset of the deformed region and are very well described by mean field calculations. The results are compared with those from other studies in beyond mean field approximations. Shape coexistence phenomena in the region of interest are discussed.

DOI: 10.1103/PhysRevC.89.014311 PACS number(s): 21.60.−n, 31.50.−x, 29.30.Kv

I. INTRODUCTION

Many physical systems undergo phase transitions. Despite the fact that atomic nuclei are finite systems, they too exhibit phase transitions, like in their shape, and these changes markedly modify the properties of the entire system. Following the introduction by Iachello [1,2] of a simple model of critical point symmetries of the shape transitions X(5) from spherical vibrator to axial rotor and E(5) from spherical to γ-unstable nuclei, there has been considerable effort invested in both theoretical and experimental studies of these dynamical symmetries. The development of collectivity as one moves away from closed shells in nuclei is a topic of abiding interest and Iachello's introduction of the X(5) critical point symmetry points the way to where one might find the critical point in such quantum phase transitions; see also reviews in Refs. [3–6].

Phase transitions have also been studied from different perspectives, using a variety of different mean field methods like the relativistic Hartree-Bogoliubov theory [7–10]. In some of these works, it was suggested that the phase transition can be related to a prolate-oblate shape transition [7,11]. In the present work we examine the issue of phase transitions in $N = 90$ isotones from a mean field perspective. In this work, triaxial deformations are taken into account, in order to describe the possible prolate to oblate shape transitions adequately if they exist. This ensures that any spurious minima corresponding to saddle points in the potential energy landscape are found. Our results reveal that the oblate minima in the $N = 90$ region are spurious and that there is no evidence for prolate oblate shape co-existence in this mass region. This result, showing that the oblate minima are saddle points in β-γ plane, is consistent with the results of Refs. [10,12].

In addition to the potential energy surfaces, the moments of inertia and quadrupole moments were calculated and compared to the experimental values. Since the issue of quantum phase transitions in a finite system is of particular interest we believe that a better understanding of these three indicators will provide deeper insight into this phenomenon. It is an open issue how nuclei in which these observables are well described by the mean field approach relate to phase transitional behaviour and/or reveal a critical point symmetry. It is well known that the cranking moment of inertia describes the structure of low and high spin yrast states rather well, provided the mean field has a well-defined, deformed shape. Thus, it is of high interest to determine the ratio $R(4/2)$ for the $N = 90$ isotones in realistic calculations. This will also allow us to establish the region in which the deformed mean field approximation is valid, i.e., the region of deformed nuclei within the mean field concept.

In the next section our calculations are described and the results are discussed. A comparison is then made with the experimental data.

The conclusions are given in Sec. III.

II. THE RESULTS

The deformed mean field for our investigation is based on a deformed Woods-Saxon potential [13] and the Strutinsky shell correction approach [14,15]. Rotational states are generated by means of the cranking approximation, which is well suited to application to deformed nuclei. Pairing correlations are included via a seniority pairing force and a double-stretched quadrupole pairing interaction. The time-odd component of the latter is of particular importance if we are to obtain a correct description of the moment of inertia [16,17]. The pairing Hamiltonian is calculated in a self-consistent fashion at each frequency and each deformation point. In order to avoid the spurious breakdown of the pairing field, approximate particle number projection via the Lipkin Nogami method is employed. For further details of the method, we refer the reader to Refs. [18,19]. The total energy is minimized with respect to the shape parameters [20]. The method has successfully been applied over the entire nuclear chart, giving in general a very accurate description of the rotational spectra of deformed nuclei; see, e.g., Refs. [21–24]. The accuracy with which the TRS calculations reproduce the properties of high spin

*ganioglu@istanbul.edu.tr

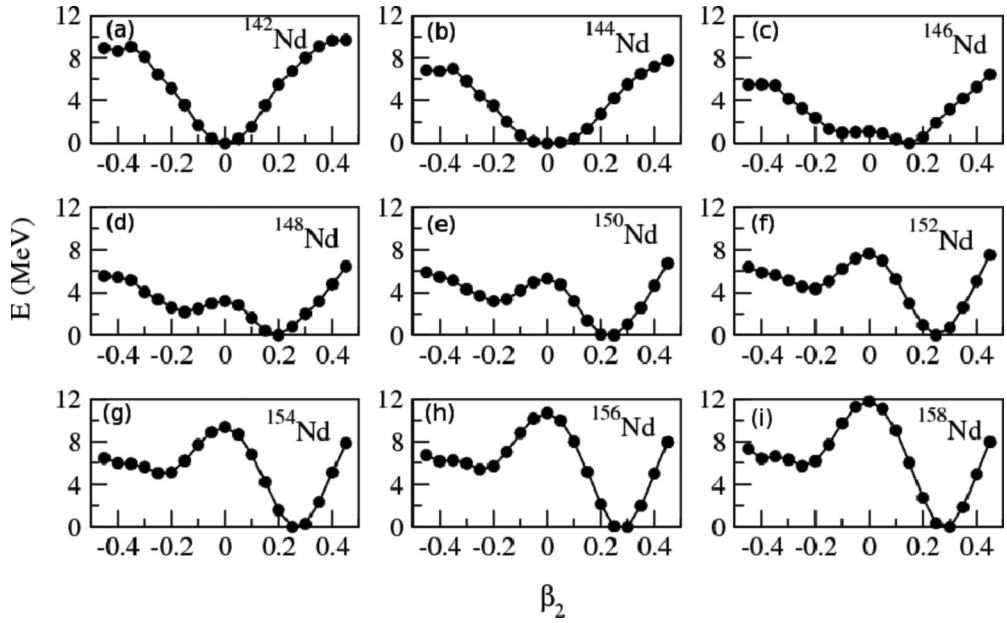

FIG. 1. Potential energy as a function of β_2 for the even-even Nd nuclei from $N = 82$–98, as a result of mean-field calculations with a deformed Woods-Saxon potential. (Details on calculations are given in the text.)

rotational bands gives us some confidence in the method when it is employed in describing the properties of deformed nuclei more generally with the mean field.

We start by examining the potential energy surfaces as they emerge from calculations for axially symmetric shapes for the chain of even-even Nd isotopes, from $N = 82$ to $N = 98$ (see Fig. 1). The potential energy curves in the Nd isotopes as a function of N might serve as a textbook example for the onset of deformation; see, e.g., Ref. [25]. The $N = 82$ isotope is spherical, and one expects a vibrational excitation structure. On the other hand, for $N = 98$ we see a well-developed deformed shape, having $\beta_2 \approx 0.28$ and hence rotational structure. At $N = 84$, the equilibrium shape is still spherical, but considerably softer. For $N = 86$, there is effectively a broad minimum and at $N = 88$ a deformed shape emerges. The deformation increases smoothly with increasing neutron number up to ^{150}Nd and there is little change above ^{150}Nd. The mean field approximation is applicable when the fluctuations in β are smaller than the mean field value, which is equivalent to stating that the zero-point motion is confined within the barriers of the potential surface. For those cases the cranking approximation is well justified. Our results indicate that for $N = 90$ this indeed is the case.

From the potential energy curves shown in Fig. 1 one may deduce that there is oblate-prolate shape coexistence in some of the Nd isotopes. By relaxing the condition of axially symmetric shapes and allowing triaxiality to play a role, one realizes that the oblate "minimum" is actually a saddle point and that there is no sign of shape coexistence (see Fig. 2). Clearly, any conclusion about prolate-oblate shape coexistence should be made with care when the symmetry is restricted to axially symmetric shapes. Oblate minima in the $N = 90$ region are an artifact of the symmetry restriction in the model. The calculations show that the $N = 90$ isotones from Nd to Dy all have well-developed minima at $\beta_2 \approx 0.23$. In order to address the question of whether a simple mean field model can give a quantitative description of nuclei at or near a critical point, we compare our calculations with the Skyrme Hartree-Fock BCS (HFBCS) calculations described in Ref. [26]. Qualitatively,

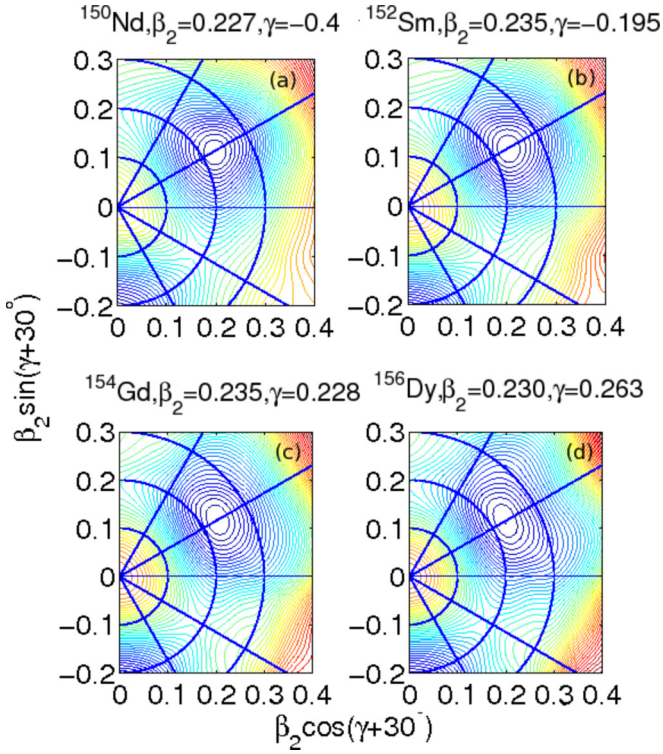

FIG. 2. (Color online) Calculated TRSs for the $N = 90$ isotones, ^{150}Nd, ^{152}Sm, ^{154}Gd, and ^{156}Dy. Energy difference between adjacent contour lines is 100 keV. The calculations were carried out with a deformed Woods-Saxon potential. (The details are given in the text.)

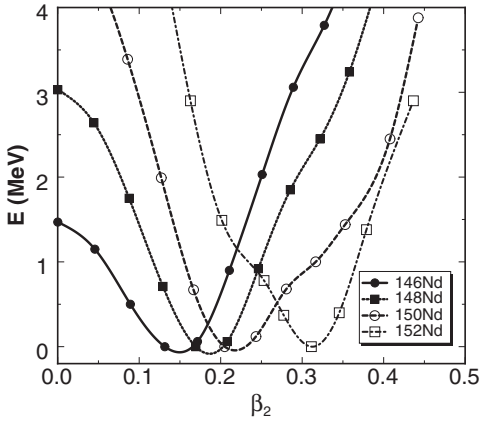

FIG. 3. Calculated potential energy as a function of β_2 for some even-even Nd isotopes as a result of Skyrm Hartree-Fock BCS (HFBCS) calculations described in Ref. [26].

the calculations are in agreement; see Fig. 3. The potential depths of the energy curves are very similar, revealing that at $N = 86$, the nuclear shape is becoming deformed with a similar value of the deformation parameter for all the values of Z. The main difference in the calculations is related to the more sudden increase in deformation between $N = 90$ and $N = 92$ in the Skyrme HFB calculations, whereas in the calculations with Woods-Saxon potential, the deformation increases smoothly with neutron number. This difference most probably reflects the difference in the single-particle spectrum, related to deformed shell gaps below and above the [660]1/2 Nilsson orbit. It is also interesting to compare our results with the Hartree-Fock-Bogoliubov (HFB) approach using the Gogny interaction [27]. As one would expect, this study gives potential energy curves in a region of interest similar to ours. They found that the transitional behavior appears for the $N = 86$–90 isotopes, $^{146-150}$Nd. The main difference is that they find a wide minimum on the prolate side as well as an additional minimum on the oblate side. As indicated earlier, the suggestion of shape coexistence should be considered with care when restricting calculations to axial symmetric shapes.

As discussed above, the potential energy surfaces reveal nicely the calculated equilibrium shapes as a function of deformation but do not allow further conclusions to be made on the applicability of the model with respect to observables such as the quadrupole moment and moments of inertia. In the deformed mean field picture, the transitional quadrupole moment is an excellent observable to characterize the shape of the nucleus. In the collective model of Bohr and Mottelson, assuming a uniformly rotating body with given spins, the transitional moment is given by

$$B(E2; K I_1 \rightarrow K I_2) = \frac{5}{16\pi} e^2 Q_0^2 \langle I_1 K 20 | I_2 K \rangle^2, \quad (1)$$

where the intrinsic quadrupole moment $Q_\circ$ is obtained as the integral of the charge distribution. One can directly use the deformation parameters of the potential to deduce the corresponding quadrupole moment. Instead, in the present calculations, we calculate the expectation values of the quadrupole operators Q_{20} and Q_{22} microscopically from the

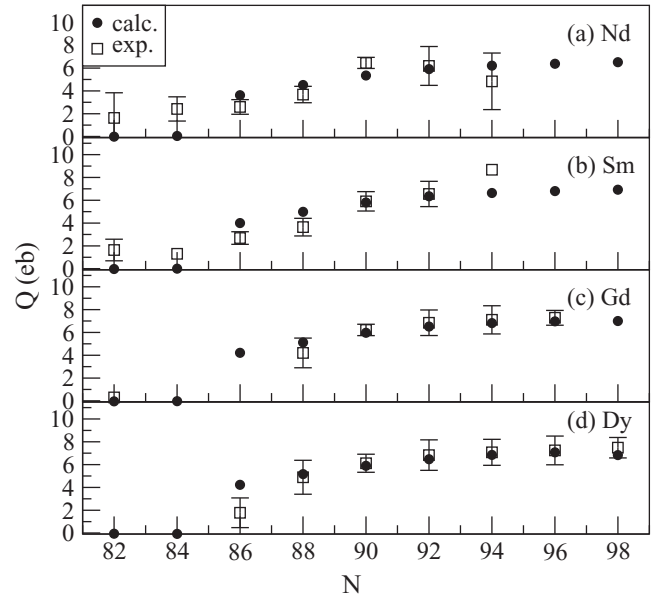

FIG. 4. The experimental (squares) [28] and calculated (circles) quadrupole moments for even-even Nd, Sm, Gd, and Dy isotopes as a function of neutron number N.

occupation probability of the single-particle levels of the Woods-Saxon potential:

$$\langle Q_{2\mu} \rangle = \mathrm{Tr}\langle q_{2\mu} \rho(\omega) \rangle, \quad (2)$$

where $q_{2\mu}$ is the matrix of the single-particle quadrupole moments and $\rho(\omega)$ is the density matrix at rotational frequency ω as obtained in the self-consistent HFB diagonalization. Reference [9] asserts that if one is to recognize a critical point symmetry in a particular nucleus, $B(E2)$ ratios are one of two properties that must be calculated. Although $B(E2)$ rates are not possible to obtain directly from the mean-field calculations, we compare our calculated quadrupole moments to the experimentally deduced ones, using the relation between experimental $B(E2)$ ratios and quadrupole moments, Eq. (1). For obvious reasons, the deformed mean field does not give a quadrupole moment when the deformation is zero. In contrast, experiment reveals a sizable moment, showing that the deformed mean field model does not apply to those nuclei in Fig. 4. (For the experimental data, see Ref. [28].) The transition probability can be calculated in, e.g., the random phase approximation (RPA), as the first-order extension of the mean field. Indeed, RPA calculations nicely depict the drop in excitation energy from $N = 82$ to $N = 84$ [29]. In our calculations, we find a sudden onset of the quadrupole moment at $N = 86$, related to the fact that the deformation has a nonzero value. This does not necessarily imply that the approximations underlying the calculations are valid. In the experiment one notices a smooth increase in the transitional quadrupole moment, revealing the transition from vibrational-like to rotational structure.

The change in the quadrupole moment with N, dq/dN, is expected to be largest at the point of transition from vibrational-like to deformed. In the chains of nuclei discussed here from Nd to Dy, it occurs between $N = 88$ and $N = 90$.

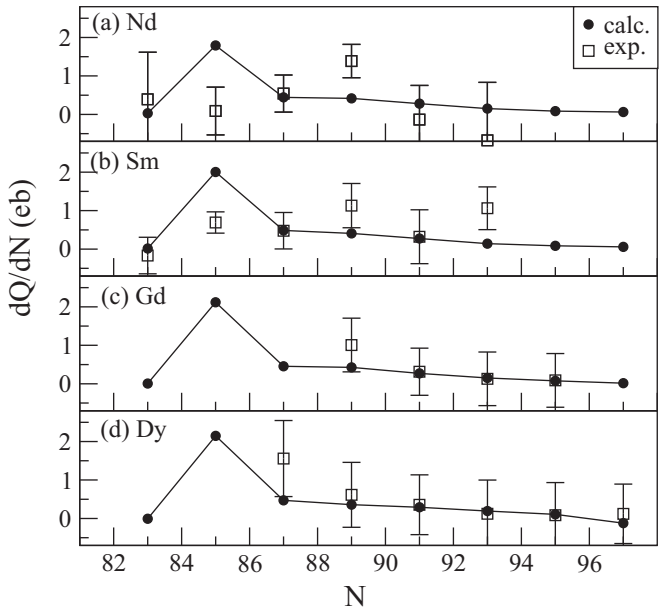

FIG. 5. The change in quadrupole moments for experiment (squares) [28] and calculations (circles) as a function of neutron number in the even-even Nd, Sm, Gd, and Dy nuclei for $N = 82$–98 nuclei from top to bottom respectively.

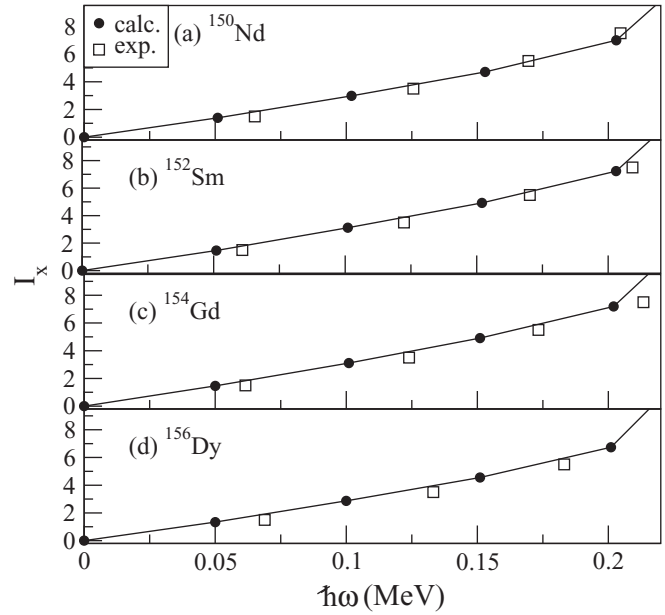

FIG. 6. The experimental (squares) [28] and calculated (circles) spin(I_x) vs rotational frequency ($\hbar\omega$) in the even-even Nd, Sm, Gd, and Dy nuclei for $N = 82$–98 nuclei from top to bottom respectively.

This result is consistent with the result of the study of the beyond mean field approximation using the Gogny interaction given in Ref. [10] (see Fig. 5). For transitional nuclei the contribution to the quadrupole transition originates from a superposition of uniform rotational and vibrational motion. Since the rotational component is larger in size, one expects that the calculations assuming uniform rotation may yield reasonable results, even when the structure of the first excited state still has an appreciable component of vibrational motion. Indeed, the calculated quadrupole moments agree rather well, starting from $N = 86$ and certainly by $N = 88$.

The calculated spins as a function of the rotational frequency, from which one can deduce the moment of inertia, are another sensitive probe of the validity of the cranking approximation. The moments of inertia are described rather well for deformed nuclei, for which the mean field approximation is valid. In Fig. 6, we compare the calculated spins to experiment for all of the $N = 90$ isotones discussed in our study. Clearly, the calculations agree very well with the experimental data in the low-spin regime, which is of relevance to our discussion. This indicates that the $N = 90$ isotones are well described by the mean field approach, indicating the validity of a static-deformed mean field.

The most sensitive probe in the comparison with experiment is the second moment of inertia, J^2. We used the calculated spin alignment and frequency values to calculate the second moment of inertia by means of the well-known equation $J^2 = dI/d\omega$ and the experimental moments of inertia were obtained from the following equation:

$$J^2 = \frac{I_x(\omega_2) - I_x(\omega_1)}{\hbar(\omega_2 - \omega_1)}. \qquad (3)$$

For an ideal vibrator, the J^2 moment of inertia is expected to be infinite. It will be very large for anharmonic vibrators. On the other hand, in a regime of deformed nuclei, we expect a smooth increase in J^2 with increasing deformation. Hence, studying the transition from vibrator to rotor in an isotopic chain, should reveal a minimum in the moment of inertia as a function of neutron number. Indeed, comparing the evolution of the moments of inertia in the different isotopic chains from Nd to Dy, it reaches a minimum at $N = 90$ and then smoothly and steadily increases for larger N values, which is seen in Fig. 7.

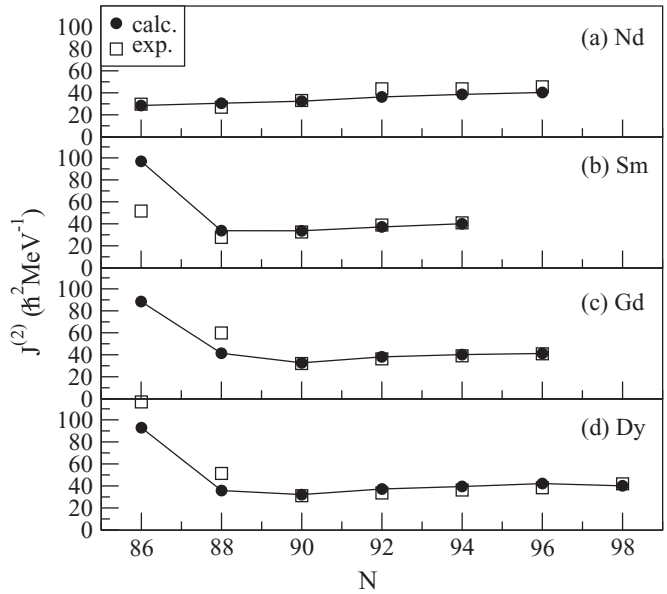

FIG. 7. The experimental (squares) [28] and calculated (circles) dynamical moments of inertia. For the even-even Nd, Sm, Gd, and Dy isotopes as a function of neutron number N.

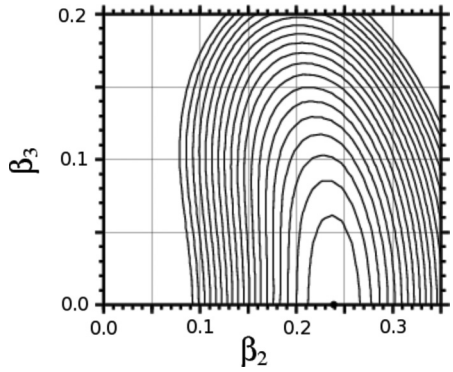

FIG. 8. Calculated octupole deformation vs quadrupole deformation for ^{150}Nd. Energy difference between adjacent contour lines is 100 keV.

Starting at $N = 90$, the moment of inertia increases smoothly, with no sign of sudden changes. The calculated second moment of inertia agree very well with experimental results from $N = 90$ onwards and show the same behavior. The reason for the larger moments of inertia in some of the $N = 88$ isotones reflects the fact that in these nuclei at these frequencies, an alignment is taking place; i.e., there is a sizable single-particle contribution to the moment. At lower frequencies, we obtain a lower moment of inertia in $N = 88$ as compared to $N = 90$, indicating that the cranking approximation has limited validity when it comes to the $N = 88$ isotones.

In order to investigate the dependence on other shape parameters, we calculated potential energy surfaces for octupole and hexadecapole deformations. For the octupole degree of freedom, one finds considerable softness that is largest at $N = 86,88$ (∼0.08–0.09)for the Nd and Sm isotopes, while it occurs at $N = 84$ (∼0.05) for the Gd and Dy isotopes. In the case of the $N = 90$ isotones the octupole softness decreases with increasing proton number, which indicates that $N = 90$ is not a major point of shape changes in the octupole direction [30]. (See Fig. 8.) Moreover, as a result of our calculations we found sizable β_4 values for $N = 90$ and $N = 92$ [31]. See Figs. 9 and 10.

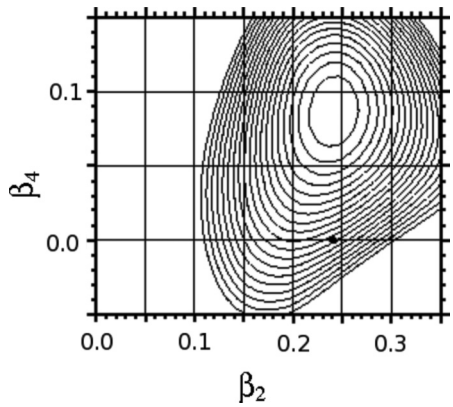

FIG. 9. Calculated hexadecapole deformation vs quadrupole deformation ^{150}Nd. Energy difference between adjacent contour lines is 100 keV.

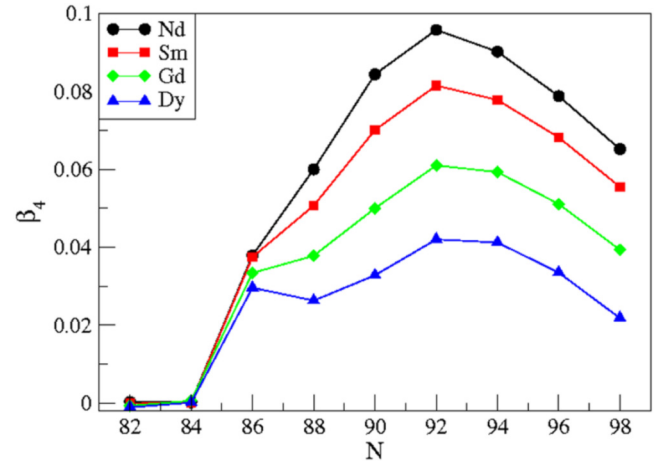

FIG. 10. (Color online) The calculated hexadecapole deformations of the even-even Nd, Sm, Gd, and Dy isotopes as a function of neutron number N.

The energy ratio $R_{4/2}$ is another important indicator of structure. We used an averaging procedure in our calculations in order to determine the $E(4)/E(2)$ ratio. First the mean field moments of inertia are calculated microscopically at each frequency. Then using the relationship between energy and moments of inertia we calculate the $R_{4/2}$ ratio in rotational basis using the following formula:

$$E_{\text{rot}} = \frac{\hbar^2}{2J} I(I+1) \tag{4}$$

and

$$E(4_1^+)/E(2_1^+) = 3{,}33\frac{J^{(2)}}{J^{(4)}}, \tag{5}$$

where $J^{(2(4))}$ is calculated at the frequency for the $2(4)^+ \rightarrow 0(2)^+$ transition, using interpolation. The calculated ratios are shown in Table I. They clearly show that the mean field estimates are consistent with the experimental data with respect to this energy ratio. The experimental energies are taken from Ref. [32].

The moment of inertia is changing with frequency, mainly due to the change in the pairing field. This effect is not negligible, particularly for the $N = 90$ isotones. Apparently, $N = 90$ nuclei are nicely described within the cranking approximation. A value of 2.9 appears to be a lower limit for the $R_{4/2}$ ratio that can be obtained in cranking calculations. The value of 3.3 obtained at the symmetry limit of SU(3) corresponds to an ideal rigid rotor. Nuclei are not rigid rotors and the change in the moment of inertia, as obtained from the cranking calculations,

TABLE I. The calculated and experimental $E(4_1^+)/E(2_1^+)$ ratio for the $N = 90$ isotones.

Nucleus	Calculated $E(4_1^+)/E(2_1^+)$	Experimental $E(4_1^+)/E(2_1^+)$
^{150}Nd	2.90	2.927
^{152}Sm	3.04	3.009
^{154}Gd	3.12	3.015
^{156}Dy	3.07	2.934

yields a rather accurate value of the response of the nuclear mean field. Pairing correlations, of course, are crucial in this context and are the single most important factor causing the increase in the moment of inertia with increasing spin. The dynamic change of pairing correlations and their influence on a possible phase transition is not considered in algebraic approaches. Therefore, one expects a "smearing effect," due to fluctuations in the nuclear wave function. It implies that the value of 2.91, as obtained for the critical point symmetry, has to be treated with caution in any comparison with real nuclei. As stated in Ref. [33], nucleon numbers take only discrete values and there is no continuous parameter associated with them. From our calculations it emerges that $N = 90$ is well described within the mean field model and that $N = 88$ and $N = 90$ mark the borderline between nuclei that can be described well within the mean field and those that reveal deficiencies. The presence of pairing correlations makes it difficult to use 2.91 as a number that definitively characterizes the phase transition in nuclei. One may assume that the value is smaller in real nuclei. In addition, the presence of pairing correlations in the ground state results in two major changes: (i) the critical value will be shifted to a lower neutron number and (ii) the phase transition is most likely to be smeared out due to the presence of strong fluctuations.

III. CONCLUSION

The present paper investigates the validity of the deformed mean field for the description of $N = 90$ isotones with pairing-deformation self-consistent total Routhian surface (TRS) calculations. In order to understand how the nuclear shape evolves, the calculations are carried out in the range of $N = 82$–98. Our results show that the two minima appearing in axially symmetric calculations correspond to a spurious one at oblate shape and a proper one at prolate shape. We compared our calculations with the Skyrme Hartree-Fock BCS (HFBCS) calculations and to previous studies in the beyond mean field approximation. Previous proposals of shape coexistence are not verified and should be considered with care when calculations are restricted to axially symmetric shapes [7,8,27]. Our calculations clearly show that the transitional region of the $N = 90$ isotones is well explained using two- and three-dimensional potential energy surfaces within the cranking approximation. The quadrupole moments, the moments of inertia, and the calculated $R_{4/2}$ ratio all agree very well with experimental results. The impact of our study for the characterization of phase transition in nuclei needs to be further elucidated. It may also indicate a restricted validity of the concept due to the presence of large fluctuations and other degrees of freedom.

ACKNOWLEDGMENTS

This project is supported by the Turkish Automic Energy Authority (TAEK) under Project No. DPT-04K120100-4.

[1] F. Iachello, Phys. Rev. Lett. **85**, 3580 (2000).
[2] F. Iachello, Phys. Rev. Lett. **87**, 052502 (2001).
[3] P. Cjenar, J. Jolie, and R. F. Casten, Rev. Mod. Phys. **82**, 2155 (2010).
[4] D. Bonatsos, D. Lenis, D. Petrellis, P. A. Terziev, and I. Yigitoglu, Bulg. J. Phys. **34**, 227 (2007).
[5] D. Bonatsos, arXiv:0807.4492v1.
[6] L. Fortunato, C. E. Alonso, J. M. Arias, and A. Vitturi, Proc. DAE Symp. Nucl. Phys. **57**, 45 (2012).
[7] R. Fossion, D. Bonatsos, and G. A. Lalazissis, Phys. Rev. C **73**, 044310 (2006).
[8] R. Rodríguez-Guzmán and P. Sarriguren, Phys. Rev. C **76**, 064303 (2007).
[9] T. Nikšić, D. Vretenar, G. A. Lalazissis, and P. Ring, Phys. Rev. Lett. **99**, 092502 (2007).
[10] T. R. Rodríguez and J. L. Egido, Phys. Lett. B **663**, 49 (2008).
[11] P. Sarriguren, R. Rodríguez-Guzmán, and L. M. Robledo, Phys. Rev. C **77**, 064322 (2008).
[12] Z. P. Li, T. Niksic, D. Vretenar, J. Meng, G. A. Lalazissis, and P. Ring, Phys. Rev. C **79**, 054301 (2009).
[13] S. Ćwiok, J. Dudek, W. Nazarewicz, J. Skalski, and T. R. Werner, Comput. Phys. Comm. **46**, 379 (1987).
[14] V. M. Strutinsky, Yad. Fiz. **3**, 614 (1966) [Sov. J. Nucl. Phys. **3**, 449 (1966)]; V. M. Strutinsky, Ark. Fys. **36**, 629 (1966); Nucl. Phys. A **95**, 420 (1967)
[15] V. M. Strutinsky, Nucl. Phys. A **122**, 1 (1968).
[16] R. Wyss and W. Satuła, Phys. Lett. B **351**, 393 (1995).
[17] W. Satuła and R. Wyss, Phys. Rev. C **50**, 2888 (1994).
[18] W. Satuła, R. Wyss, and P. Magierski, Nucl. Phys. A **578**, 45 (1994).
[19] W. Satuła and R. Wyss, Phys. Script. **T56**, 159 (1995).
[20] R. Wyss, W. Satula, W. Nazarewicz, and A. Johnson, Nucl. Phys. A **511**, 324 (1990).
[21] D. Rudolph, C. Baktash, C. J. Gross, W. Satula, R. Wyss, I. Birriel, M. Devlin, H. Q. Jin, D. R. LaFosse, F. Lerma, J. X. Saladin, D. G. Sarantites, G. N. Sylvan, S. L. Tabor, D. F. Winchell, V. Q. Wood, and C. H. Yu, Phys. Rev. C **56**, 98 (1997).
[22] F. Lerma, M. Devlin, D. R. LaFosse, D. G. Sarantites, R. Wyss, C. Baktash, R. M. Clark, I. Y. Lee, A. O. Macchiavelli, R. W. MacLeod, D. Soltysik, and S. L. Tabor, Phys. Rev. Lett. **83**, 5447 (1999).
[23] K. Lagergren, B. Cederwall, T. Bäck, R. Wyss, E. Ideguchi, A. Johnson, A. Atac, A. Axelsson, F. Azaiez, A. Bracco, J. Cederkäll, Z. Dombradi, C. Fahlander, A. Gadea, B. Million, C. M. Petrache, C. Rossi-Alvarez, J. A. Sampson, D. Sohler, and M. Weiszflog, Phys. Rev. Lett. **87**, 022502 (2001).
[24] F. R. Xu, R. Wyss, and P. M. Walker, Phys. Rev. C **60**, 051301 (1999).
[25] W. Nazarewicz, J. Dudek, R. Bengtsson, and I. Ragnarsson, Nucl. Phys. A **435**, 397 (1985).
[26] S. Goriely, M. Samyn, M. Bender, and J. M. Pearson, Phys. Rev. C **68**, 054325 (2003).

[27] L. M. Robledo, R. R. Rodriguez-Guzman, and P. Sarriguren, Phys. Rev. C **78**, 034314 (2008).
[28] http://www.journals.elsevier.com/nuclear-data-sheets
[29] E. Ganioğlu *et al*. (unpublished).
[30] P. A. Butler and W. Nazarewicz, Rev. Mod. Phys. **68**, 349 (1996).
[31] E. Ganioğlu and R. Wyss, AIP Conf. Proc. **899**, 111 (2007).
[32] http://nndc.bnl.gov
[33] R. F. Casten and N. V. Zamfir, Phys. Rev. Lett. **87**, 052503 (2001).